



A Structured-Population Model of *Proteus*  
*mirabilis* Swarm-Colony Development

Bruce P. Ayati

SMU Math Report 2004-04

DEPARTMENT OF MATHEMATICS  
SOUTHERN METHODIST UNIVERSITY

# A Structured-Population Model of *Proteus mirabilis* Swarm-Colony Development

Bruce P. Ayati

January 29, 2022

## Abstract

In this paper we present continuous age- and space-structured models and numerical computations of *Proteus mirabilis* swarm-colony development. We base the mathematical representation of the cell-cycle dynamics of *Proteus mirabilis* on those developed by Esipov and Shapiro, which are the best understood aspects of the system, and we make minimum assumptions about less-understood mechanisms, such as precise forms of the spatial diffusion. The models in this paper have explicit age-structure and, when solved numerically, display both the temporal and spatial regularity seen in experiments, whereas the Esipov and Shapiro model, when solved accurately, shows only the temporal regularity.

The composite hyperbolic-parabolic partial differential equations used to model *Proteus mirabilis* swarm-colony development are relevant to other biological systems where the spatial dynamics depend on local physiological structure. We use computational methods designed for such systems, with known convergence properties, to obtain the numerical results presented in this paper.

**Key words:** *Proteus mirabilis*, swarm colony, age structure, space structure, partial differential equations .

## 1 Introduction

In this paper we present continuous age- and space-structured models and numerical computations of *Proteus mirabilis* swarm-colony development. *Proteus mirabilis* has received treatment in the mathematical biology literature due to the strikingly regular spatial-temporal

patterns swarm colonies make on an agar surface [44, 49]. Not only do the swarm colonies form regularly spaced concentric terraces in a bulls-eye pattern, but the total time taken to form a ring is invariant under changes in the agar or glucose concentration in the substrate.

The invariance of the total cycle time rules out chemotaxis as an explanation for the ring formation, as do biological observations of *Proteus* responses to chemical stimuli [49]. Esipov and Shapiro [16] saw that the regularity of the ring-formation cycle is a result of the regularity of the differentiation-dedifferentiation cycle of individual bacteria. The resulting model was an equation that is first-order hyperbolic in the age variable (also called a kinetic or transport term) and nonlinear parabolic in space.

This mathematical explanation for swarm-colony behavior necessarily differs from chemotaxis models, such as those for swarm-colony formation in *E. coli*, due to the temporal invariance of the *Proteus* system [40].

*Proteus* has been suggested as a model system for problems in morphogenesis and other complex self-organizing systems [16, 39, 44], but it is also an example of a biological system where the local kinetics – the age structure – determine the spatial dynamics of the system. *Dictostelium* has received much treatment as a model system for other problems in morphogenesis [22]. The study of *Proteus* can have similar relevance to systems such as tumor growth [5, 15, 43] and natural forests [7, 27, 28, 30], where physiological structure, such as age, size or activation levels in tumor and immune cells, can play an important role in the spatial behavior of the system. Bertuzzi and Gandolfi [6] presented a cancer tumor-cord model with both space and size structure with some similarity to the kinetics in the *Proteus* models, although they did not present results for their full model.

We base the models of *Proteus* swarm-colony development in this paper on models presented in [16]. Due to the phonetic and conceptual similarities of the terms “swimmer” and “swarmer”, we depart from standard terminology and use the term “dividing cell” instead

of “swimmer cell”. This change in terminology emphasizes both the nonmotile character of the dividing cells on an agar surface and the fact that the swarmer cells are filaments<sup>1</sup>.

The models in [16] indicated that experimental study of sharp dedifferentiation in *Proteus* might yield insight into their periodic swarm-colony development. Dedifferentiation, also called septation, is the process in which multinuclear swarmer cells subdivide into mononuclear dividing cells. This experimental study remains important for the models in this paper, but perhaps more critical are experiments that determine how the lag phase in differentiation – the process in which mitosis of dividing cells results in a swarmer cell rather than two dividing cells – affects swarm-colony development, and ideally give the functional forms of this lag. This lag in the onset of differentiation was identified in [49], and is an important part of the models in this paper and of those in [39], but is not used in [16].

We begin the paper with a description of *Proteus* swarm-colony development and aspects of the relevant biology, and then discuss differences between the models in this paper and prior work. When referring to the Esipov-Shapiro system, we mean a modified form of the system formally presented in [16]. Without these changes, the Esipov-Shapiro system has no swarming behavior at all and is thus not really a model of the swarm-colony development. In Appendix A, we elaborate upon the changes and why they might reflect the intended mechanisms of Esipov and Shapiro. Again, without these changes, we can have no useful discussion of their model.

The most significant difference between the models in this paper and those in [16] is that the models in this paper reproduce the spatial regularity seen in *Proteus* swarm colony development, whereas, when solved accurately, the Esipov-Shapiro system, even when modified with the maximum benefit of doubt, does not. The damping in terrace width is discussed in

---

<sup>1</sup>James Shapiro at the University of Chicago suggested this terminology when discussing the behavior of *Proteus* on an agar surface.

more detail in Appendix A.

In subsequent sections, we present our mathematical models, the numerical methodology used to solve the age-, space- and time-dependent systems, and the results from the numerical computations.

## 2 *Proteus mirabilis* Swarm-Colony Development

When inoculated onto an agar surface, *Proteus* begin formation of strikingly regular spatio-temporal patterns that begin with three initial phases: a lag phase, a first swarming phase, and a first consolidation phase; these form what appear to be the center circle and first ring of a bulls-eye. This is followed by repeating cycles of ring, or terrace, formation that consist of a swarming phase followed by a consolidation phase. These subsequent terraces are equal in width and time of formation. Perhaps most interestingly, the time of terrace formation is invariant under changes in the glucose or agar concentration of the substrate, although changes in agar concentration do affect the ratio of time spent swarming versus consolidating, and changes in glucose increase terrace width. Terrace formation does vary by temperature [44].

Broth cultures of *Proteus* consist of mononuclear cells (often called “swimmer” cells, but in this paper called “dividing” cells) about  $0.6 \mu\text{m}$  wide and  $1\text{-}2 \mu\text{m}$  long with short flagella. On an agar surface these cells lengthen somewhat to about  $0.8 \mu\text{m}$  wide and  $2\text{-}4 \mu\text{m}$  long. After a period of time<sup>2</sup>, some cells near the perimeter begin to lengthen into multinuclear filament cells (called “swarmer cells”) that reach sizes of  $0.7 \mu\text{m}$  wide and  $20\text{-}80 \mu\text{m}$  long. The swarmer cells have longer flagella than the dividing cells. Moreover, dividing cells normally have between 1 to 10 flagella, whereas swarmer cells have between 500 to 5000, a 10-fold

---

<sup>2</sup>This time-lag before swarmer cell production begins is incorporated into the models in this paper and in [39] as a lag in density, but is not used in [16].

increase in the number of flagella per cubic micrometer of bacterial volume [49]. The process in which dividing cells become swarmer cells is called “differentiation.” Differentiation only occurs above one dividing-cells density and below another.

It is the swarmer cells that move across the agar during the swarming phase. The movement of swarmer cells on the agar surface is a complex process. The swarmers use their elongated flagella to move in fluid extracted by them from the agar gel. They do so in groups, or “rafts” [16]. Consequently, the unit of random motion in any diffusion approximation of *Proteus* movement is a large and complicated entity.

When the multinuclear swarmer cells approach a maximum size, they rapidly break down into single-nucleus dividing cells. This process is called “dedifferentiation.” Since mitosis results in exponential growth, the size of a swarmer cell is an exponential weight times its age. Thus, dedifferentiation occurs when swarmers reach a maximum age.

Varying glucose concentration greatly alters biomass production without greatly affecting the spatial or temporal aspects of the swarm and the consolidation cycle of terrace formation. Thus, the cycle is not affected by biomass. Changes in agar concentration do not change the total time of terrace formation, but higher agar concentrations shorten the time spent swarming and the width of the terraces, and lengthen the time spent in consolidation [16].

### **3 Differences and Commonalities with Previous Models**

Models presented in this paper differ from models presented in [16] in several respects. We use a radially symmetric geometry with no-flux boundary conditions, as would be the case on a petri dish. Models used in [16] use a linear geometry. We use a diffusion approximation which arises from isotropic random motion instead of Fickian diffusion [1, 24, 41]. An additional difference between the models in this paper and in [16] is that we present results

for nondimensionalized models.

The most substantial differences between the models presented here and in [16] are in the different forms of the diffusivity,  $D$ , and the differentiation rate to swarmer cells,  $\xi$  (as will be discussed in Section 5, our numerical treatments also differ, with nontrivial consequences.) The diffusivity in [16] relied on a memory field: the diffusivity changes depending if the cells are in a collective state of motion or at rest. This is not clearly supported biologically and, invoking Occam's Razor, is not used in the models in this paper, since it is not needed. Also, the diffusivity in [16] depends on the dividing-cell population.

The diffusivity in this paper depends only on swarmer biomass. Since we use swarmer biomass rather than swarmer numerical density in the diffusivity, the exponential weighting from mitosis that describes size means that younger swarmer cells do not contribute as much as older swarmer cells. This weighting also models the fact that each nucleus of a swarmer cell dedifferentiates into a dividing cell. Because of this weighting, age-structured models of *Proteus* swarm-colony development presented in this paper can also be thought of as size-structured.

The second and most important difference, the form of  $\xi$ , is based on incorporating the property that dividing cells do not form swarmer cells until a minimum population density is reached, a mechanism discussed in [49] and introduced in models in [39], but not used in [16]. This threshold is represented mathematically by setting  $\xi$  to zero for low dividing-cell densities.

We focus on three features of *Proteus* swarm-colony development: cycle regularity, ring-width uniformity, and control of the ratio of swarm to consolidation time. A regular cycle does occur in the Esipov-Shapiro system, and these authors are able to control the ratio of swarm time to consolidation time. However, the terrace width decreases from cycle to cycle, so the front velocity does not remain periodic, as shown in Appendix A.

In [16] it was concluded that models that used a sharp age of septation from swarmer filament to dividing cells gave periodic front dynamics, whereas a constant dedifferentiation rate did not.

Medvedev, Kaper, and Kopell [39] developed a reaction-diffusion model of *Proteus* swarm-colony development based on averaging over the age variable. The model relied on a specific nonlinear form of the diffusivity to produce periodic front dynamics. In [39], a constant dedifferentiation rate was used rather than a sharp age of septation. To obtain a periodic front velocity, the models in [39] also introduced a piecewise constant differentiation rate with a lag phase – a biological mechanism mentioned in [49] and used in the models in this paper – and a diffusivity dependent on the ratio of swarmer-cell to dividing-cell biomass. The use of a constant dedifferentiation rate allowed the age-structured diffusion system to be reduced to a reaction–diffusion system. This reduction has advantages both numerically and analytically. Moreover, a reaction-diffusion equation with periodic front dynamics is an interesting mathematical object in its own right. However, removing explicit age eliminated a mechanism for controlling the ratio of time spent swarming to time spent in consolidation without changing the total cycle time. No mechanism within the reaction-diffusion framework was suggested to replace this.

The biological mechanisms that are best understood are emphasized in the models in this paper. In particular, we maintain the explicit age structure. Due to experimental results<sup>3</sup> which postdate previous work [16, 39], we are more confident in assuming a sharp age of septation. New numerical methods for handling age-structured population models with nonlinear diffusion have been developed so that computations that incorporate the known properties of *Proteus* swarm-colony development can be run efficiently [2, 3].

---

<sup>3</sup>Preliminary experiments conducted by James Shapiro’s laboratory at the University of Chicago suggest that *Proteus mirabilis* that have been genetically modified to no longer have a sharp septation age lose periodicity in their swarm-colony development.

Because less is known about the specific forms of the diffusion and diffusivity, we attempt to use the simplest form of diffusivity suitable for this system. Rather than using a relatively complicated fractional form involving both swarmer and dividing cells, we use a diffusivity that is proportional to swarmer biomass above a threshold, reflecting the need for swarmers to group together in order to move. This is the simplest form that is biologically justified and that results in both swarming and consolidation. This density dependence on swarmers, due to “raft” building, is not unique to the models in this paper and is also used in [16] and [39]. The diffusivity we use, since  $\xi$  is zero above some threshold, also results in an absence of swarmers in the interior of the colony – the primary justification for the dependence of the diffusivity on dividing cells in the other models.

The different model mechanisms and results for those in this paper, Esipov-Shapiro, and Medvedev et al. are summarized in Table 1. The models in this paper are unique in reproducing three major aspects of *Proteus* swarm-colony development: temporal regularity of overall cycle time, spatial regularity, and control of the ratio of swarm time to consolidation time. Moreover, by retaining the explicit age structure in the mathematics, the models reproduce the colony behavior by relying on only two main mechanisms.

## 4 The Model

The models in this paper and in [16] are based on a mathematical framework with some history behind it. Skellam [46] considered the effects of diffusion on populations in his classic work of 1951. Sharpe and Lotka in 1911 and McKendrick in 1926 considered population models with linear age structure [48]. More recently, Gurtin and MacCamy [20] considered models with nonlinear age structure. Rotenberg [45] and Gurtin [19] posed models dependent on both age and space. Gurtin and MacCamy [21] differentiated between two kinds of diffusion in these models: diffusion due to random dispersal, and diffusion toward an area

Mechanism \ Model	Ayati	Esipov-Shapiro	Medvedev et al.
Dependence of diffusivity on swarmer density	✓	✓	✓
Dependence of diffusivity on dividing-cell density		✓	✓
Memory field		✓	
Lag phase in $\xi$	✓		✓
Explicit age structure	✓	✓	
Behavior \ Model	Ayati	Esipov-Shapiro	Medvedev et al.
Regularity of swarm and consolidation cycle	✓	✓	✓
Regularly spaced concentric terraces	✓		✓
Control of ratio of swarm to consolidation time	✓	✓	

Table 1: Mechanisms and behaviors for different models of *Proteus* swarm-colony development. The models in this paper are unique in reproducing three major aspects of the colony development, and, by retaining the explicit age structure, reproduce the colony behavior with only two main mechanisms.

of less crowding. Existence and uniqueness results can be found for various forms of these models in Busenberg and Iannelli [8], di Blasio [13], di Blasio and Lamberti [14], Langlais [33], and MacCamy [37]. Further analysis has been done by several authors [23, 31, 34, 38].

For our model, we assume the colony is radially symmetric. The variables  $r$ ,  $a$ , and  $t$  represent radius in two-dimensional space, age, and time, respectively. The function  $u(r, a, t)$  represents the swarmer-cell population density at radius  $r$ , age  $a$ , and time  $t$ . The functions  $p(r, t)$  and  $v(r, t)$  represent the biomass density of swarmer cells and the dividing-cell population density, respectively, at radius  $r$  and time  $t$ . The dividing-cell population density,  $v$ , is measured in population-density units (pdu) with  $\text{pdu} = \text{Gc}/\text{cm}^2$ , where Gc denotes one billion cells. The swarmer-cell population density,  $u$ , is measured in pdu/hr. The swarmer-cell biomass density,  $p$ , is measured in  $\text{mg}/\text{cm}^2$ .

The dimensional model consists of the age-structured nonlinear diffusion system

$$\partial_t u + \partial_a u = \frac{1}{r} \partial_r (r \partial_r (D(p)u)) - \mu(a)u, \quad 0 \leq r < r_m, \quad a > 0, \quad t > 0, \quad (4.1a)$$

$$\partial_t v = \frac{1 - \xi(v)}{\tau} v + \int_0^\infty \mu(a) u e^{a/\tau} da, \quad 0 \leq r \leq r_m, \quad t > 0, \quad (4.1b)$$

$$u(r, 0, t) = \frac{\xi(v)}{\tau} v(r, t), \quad 0 \leq r \leq r_m, \quad t > 0 \quad (4.1c)$$

with boundary and initial conditions

$$\partial_r (D(p(r_m, t))u(r_m, a, t)) = 0, \quad a > 0, \quad t > 0, \quad (4.1d)$$

$$u(r, a, 0) = 0, \quad 0 \leq r \leq r_m, \quad a \geq 0, \quad (4.1e)$$

$$v(r, 0) = v_0(r), \quad 0 \leq r \leq r_m. \quad (4.1f)$$

The parameter  $\tau$  is the time it takes a cell to subdivide. A typical value of  $\tau$  is 1.5 hours.

The total motile swarmer cell biomass is given by

$$p(r, t) = m_0 \int_{a_{\min}}^\infty u(r, a, t) e^{a/\tau} da, \quad 0 \leq r \leq r_m, \quad t \geq 0, \quad (4.1g)$$

where  $m_0$  is measured in mg/Gc. A dividing cell has a volume of approximately  $2 \times 10^{-18} \text{m}^3$  so that  $m_0 \approx 2$  for *Proteus mirabilis*.

*Proteus* move through a process of raft building that requires two things: sufficient maturity in swarmer cells to contribute to raft building, and a sufficient biomass of mature cells to form the rafts. The lower limit of integration,  $a_{\min}$ , is the minimum age when a swarmer cell is sufficiently large, with sufficiently long flagella, to contribute to motion on the agar surface. The parameter  $a_{\min}$  is comparable to the parameter  $\theta_{\min}$ , the lower limit of integration in the total swarmer numerical density, in [16]. Each parameter controls the ratio of swarm time to consolidation time without changing the total time of ring formation. The parameter  $a_{\min}$  is related to agar concentration. The higher the concentration, the drier the surface, raising the value of  $a_{\min}$ . Higher agar concentration, and thus higher  $a_{\min}$ , shortens the swarming phase and lengthens the consolidation phase in terrace formation.

The diffusivity has the form

$$D(r, t) = D_0 \max \{ (p(r, t) - p_{\min}), 0 \}. \quad (4.1h)$$

The parameter  $p_{\min}$  is the minimum biomass needed for swarmer cells to build rafts capable of moving on the agar surface, and is roughly equivalent to  $P_{s, \min}$  in [16].

We use a differentiation function with a lag phase that is a  $C^1$  piecewise cubic with support of length  $2v_w$ :

$$\xi(v) = \begin{cases} \xi_0 \left( 2 \left( \frac{|v-v_c|}{v_w} \right)^3 - 3 \left( \frac{v-v_c}{v_w} \right)^2 + 1 \right), & |v - v_c| \leq v_w, \\ 0, & \text{otherwise,} \end{cases} \quad (4.1i)$$

The interval  $[v_c - v_w, v_c + v_w]$  is the swarmer-cell production window. The parameter  $v_c$  represents the lag phase in swarmer-cell production [39]. We use a compactly supported cubic function because it is smooth. The important aspects of the functional form of  $\xi$  are that it is zero above and below certain thresholds. Appendix B shows that the nature of the

results do not depend strongly on the shape of the curve. The shape of the curve does help with numerical issues concerning the degenerate diffusion. The parameter  $v_c$  has no analog in [16].

The dedifferentiation modulus, with a spread parameter  $\sigma$ , is

$$\mu(a) = \frac{\mu_1}{\sigma} \exp((a - a_{\max})^2/(2\sigma^2)) + \frac{\mu_2}{\sigma} H(a), \quad (4.1j)$$

where

$$H(a) = \begin{cases} 1, & a \geq 0, \\ 0, & a < 0 \end{cases}$$

is the Heaviside function. This dedifferentiation modulus represents a situation where the probability of dedifferentiation is low for young swarms, increases as they approach  $a_{\max}$  in age, and remains high afterwards. Experiments indicate that this type of dedifferentiation is dominant for *Proteus mirabilis*, and that the transition, from virtually no probability of dedifferentiation to an extremely high probability of dedifferentiation as a function of age, occurs very rapidly near the critical age,  $a_{\max}$ . Preliminary results from James Shapiro's laboratory at the University of Chicago show that different strains of *Proteus* with less sharp dedifferentiation have oscillatory, but not strictly periodic, front velocities.

We take the initial condition to be

$$v_0(r) = \begin{cases} v_h \left( 2 \left( \frac{r}{r_0} \right)^3 - 3 \left( \frac{r}{r_0} \right)^2 + 1 \right), & 0 \leq r \leq r_0, \\ 0, & r > r_0. \end{cases} \quad (4.1k)$$

Again, it is mass, not shape, that matters qualitatively. Shape effects numerical efficiency.

In the limit  $\sigma \rightarrow 0$ , which represents a sharp age at which all dedifferentiation occurs, we have a system on a bounded age domain

$$\partial_t u + \partial_a u = \frac{1}{r} \partial_r (r \partial_r (D(p)u)), \quad 0 \leq r < r_m, 0 < a < a_{\max}, t > 0, \quad (4.2a)$$

$$\partial_t v = \frac{1 - \xi(v)}{\tau} v + u(r, a_{\max}, t) e^{a_{\max}/\tau}, \quad 0 \leq r \leq r_m, t > 0, \quad (4.2b)$$

$$p(r, t) = m_0 \int_{a_{\min}}^{a_{\max}} u e^{a/\tau} da, \quad 0 \leq r \leq r_m, t \geq 0 \quad (4.2c)$$

with conditions

$$u(r, 0, t) = \frac{\xi(v)}{\tau}v(r, t), \quad 0 \leq r \leq r_m, \quad t > 0, \quad (4.2d)$$

$$\partial_r(D(p(r_m, t))u(r_m, a, t)) = 0, \quad 0 < a < a_{\max}, \quad t > 0, \quad (4.2e)$$

$$u(r, a, 0) = 0, \quad 0 \leq r \leq r_m, \quad 0 \leq a < a_{\max}, \quad (4.2f)$$

$$v(r, 0) = v_0(r), \quad 0 \leq r \leq r_m, \quad (4.2g)$$

## 4.1 A Nondimensional Model

We nondimensionalize Equations (4.1a)-(4.1k). We scale age and time by  $\tau$  and space by  $r_m$  and introduce the independent variables

$$\hat{r} = r/r_m, \quad \hat{a} = a/\tau, \quad \hat{t} = t/\tau.$$

We scale the dependent variables,

$$U(\hat{r}, \hat{a}, \hat{t}) = u(r, a, t)/(v_w/\tau), \quad V(\hat{r}, \hat{t}) = v(r, t)/v_w, \quad P = p/(m_0v_w).$$

We use the dimensionless parameters

$$\hat{D}_0 = D_0m_0v_w\tau/r_m^2, \quad P_{\min} = p_{\min}/(m_0v_w), \quad V_c = v_c/v_w,$$

$$\hat{a}_{\max} = a_{\max}/\tau, \quad \hat{a}_{\min} = a_{\min}/\tau, \quad \hat{\sigma} = \sigma/\tau.$$

We note that in this nondimensionalization, the length of the swarmer-cell production window ( $2v_w$ ) and swarmer-cell swarm threshold ( $p_{\min}$ ) are related. It seems intuitive that halving one is equivalent to doubling the other. The effect of a lag in swarmer cell production ( $v_c$ ) is isolated from the effects of  $v_w$  and  $p_{\min}$ .

For  $\hat{\sigma} \neq 0$ , we obtain the system

$$\partial_{\hat{t}}U + \partial_{\hat{a}}U = \frac{1}{\hat{r}}\partial_{\hat{r}}(\hat{r}\partial_{\hat{r}}(\hat{D}(P)U)) - \hat{\mu}(\hat{a})U, \quad 0 \leq \hat{r} < 1, \quad \hat{a} > 0, \quad \hat{t} > 0, \quad (4.3a)$$

$$\partial_{\hat{t}}V = (1 - \hat{\xi}(V))V + \int_0^\infty \hat{\mu}(\hat{a})U e^{\hat{a}} d\hat{a}, \quad 0 \leq \hat{r} \leq 1, \quad \hat{t} > 0, \quad (4.3b)$$

$$P(\hat{r}, \hat{t}) = \int_{\hat{a}_{\min}}^\infty U(\hat{r}, \hat{a}, \hat{t})e^{\hat{a}} d\hat{a}, \quad 0 \leq \hat{r} \leq 1, \quad \hat{t} \geq 0 \quad (4.3c)$$

with conditions

$$U(\hat{r}, 0, \hat{t}) = \hat{\xi}(V)V(\hat{r}, \hat{t}), \quad 0 \leq \hat{r} \leq 1, \quad \hat{t} > 0, \quad (4.3d)$$

$$\partial_{\hat{r}}(\hat{D}(P(1, \hat{t}))U(1, \hat{a}, \hat{t})) = 0, \quad \hat{a} > 0, \quad \hat{t} > 0, \quad (4.3e)$$

$$U(\hat{r}, \hat{a}, 0) = 0, \quad 0 \leq \hat{r} \leq 1, \quad \hat{a} \geq 0 \quad (4.3f)$$

$$V(\hat{r}, 0) = v_0(r_m \hat{r})/v_w, \quad 0 \leq \hat{r} \leq r_m, \quad (4.3g)$$

where

$$\hat{D}(\hat{r}, \hat{t}) = \hat{D}_0 \max \{(P(\hat{r}, \hat{t}) - P_{\min}), 0\}, \quad (4.3h)$$

$$\hat{\xi}(V) = \begin{cases} \xi_0 (2|V - V_c|^3 - 3(V - V_c)^2 + 1), & |V - V_c| \leq 1, \\ 0, & \text{otherwise,} \end{cases} \quad (4.3i)$$

$$\hat{\mu}(\hat{a}) = \frac{\hat{\mu}_1}{\hat{\sigma}} \exp((\hat{a} - \hat{a}_{\max})^2/(2\hat{\sigma}^2)) + \frac{\hat{\mu}_2}{\hat{\sigma}} H(\hat{a}). \quad (4.3j)$$

In the limit  $\hat{\sigma} \rightarrow 0$  we have the system

$$\partial_{\hat{t}}U + \partial_{\hat{a}}U = \frac{1}{\hat{r}}\partial_{\hat{r}}(\hat{r}\partial_{\hat{r}}(\hat{D}(P)U)), \quad 0 \leq \hat{r} < 1, \quad 0 < \hat{a} < \hat{a}_{\max}, \quad \hat{t} > 0, \quad (4.4a)$$

$$\partial_{\hat{t}}V = (1 - \hat{\xi}(V))V + U(\hat{r}, \hat{a}_{\max}, \hat{t})e^{\hat{a}_{\max}}, \quad 0 \leq \hat{r} \leq 1, \quad \hat{t} > 0, \quad (4.4b)$$

$$P(\hat{r}, \hat{t}) = \int_{\hat{a}_{\min}}^{\hat{a}_{\max}} U e^{\hat{a}} d\hat{a}, \quad 0 \leq \hat{r} \leq 1, \quad \hat{t} \geq 0, \quad (4.4c)$$

with conditions

$$U(\hat{r}, 0, \hat{t}) = \hat{\xi}(V)V(\hat{r}, \hat{t}), \quad 0 \leq \hat{r} \leq 1, \hat{t} > 0, \quad (4.4d)$$

$$\partial_{\hat{r}}(\hat{D}(P(1, \hat{t}))U(1, \hat{a}, \hat{t})) = 0, \quad 0 < \hat{a} < \hat{a}_{\max}, \hat{t} > 0, \quad (4.4e)$$

$$U(\hat{r}, \hat{a}, 0) = 0, \quad 0 \leq \hat{r} \leq 1, 0 < \hat{a} < \hat{a}_{\max}, \quad (4.4f)$$

$$V(\hat{r}, 0) = v_0(r_m \hat{r})/v_w, \quad 0 \leq \hat{r} \leq 1. \quad (4.4g)$$

In this paper we will examine only the limiting case of  $\hat{\sigma} \rightarrow 0$ , which corresponds to the case of a sharp age of septation, “Model A”, in [16]. The models used in the computations in this paper are nondimensional, whereas dimensional models were used in [16].

As mentioned earlier, there are two major differences between the models in this paper and those in [16]. First, the diffusivity is of much simpler form, with no memory field, and hence no parameter for the upper threshold for diffusion in a memory field ( $P_{\max}$ ). Second, there is a lag phase in the dedifferentiation function,  $\xi$ . Also, we use biomass, not numerical density (which was how the model was stated in [16]) as the relevant measure of the totality of swarms. Other differences include radial symmetry, and diffusion based on isotropic random motion rather than Fickian diffusion.

When solved accurately, these differences yield the temporal regularity seen in *Proteus* experiments, as well as the regularly spaced concentric terraces, something not seen in accurate computations of the Esipov-Shapiro system.

## 5 Numerical Methodology

There has been much investigation into numerical methods for solving models with just age structure [9, 17, 32, 36, 47]. Kim [25], Kim and Park [26], and Lopez and Trigiante [35] developed methods for age-structured populations that undergo random dispersal in space. All these methods involve uniform time and age discretizations, with the age step chosen

to equal the time step. These methods discretized along characteristics, but they did so simultaneously in age and time and thus imposed the often crippling constraint that the time and age steps must be both constant and equal. The difficulty with this approach is twofold. First, the use of constant age and time steps prevents adaptivity of the discretization in age or, especially, time. Second, and more important, the coupling of the age and time meshes can cause great losses of efficiency, since only rarely will the dynamics in time be on the same scale as the dynamics in age. This is particularly the case when space is involved, since sharp moving fronts can require small time steps, whereas the behavior in the age variable can remain relatively smooth.

The methods used in this paper [2, 3] use a moving age discretization that allows for nonuniform age and time discretizations. The age step need not equal the time step. Instead, the positions of the age nodes are adjusted by the time step. The methods preserve the important fact that age and time advance together. The age discretizations presented in [25, 26, 35] can be viewed as special cases of the methods presented in [2, 3] by setting the time and age meshes to be constant and equal and using a backward Euler discretization in time and a piecewise constant finite element space in age.

The importance of allowing different age and time discretizations is somewhat illustrated by the application of the methods of de Roos [10]. These methods have found use in the study of ecological systems such as *Daphnia* (see [11] and the references therein) as well as in theoretical population biology [29, 42]. The methods of de Roos are formulated for the case of time and a variable representing some sort of physiological structure, most simply age, and involve moving the age nodes along characteristics. They have not been formulated for explicit space. The representation of the approximate solution is probabilistic and not functional, and birth and death are handled differently than in the methods in [2, 3]. Even so, it would be interesting to know if an energy analysis could provide a framework for the

convergence analysis sought in [12]. The main effect of de Roos's methods is to separate the age and time discretizations, thereby yielding an approximation that is dispersion free in age, in order to provide a method that works in practice.

We emphasize the importance of reliable numerics. In the systems presented in this paper and in [16], the regularity in terrace formation is due to the regularity in the aging of the swarmer cells. A coarse, stage-structured numerical approximation to the continuous aging term, such as that used in [16], can constitute a qualitatively different swarmer-cell life cycle than that of the original continuous model. Also, the degenerate diffusion can be altered by the choice of the time step. The numerical computation may then show periodic front dynamics that are not obtained by an accurate solution of the original continuous equations, but are induced by a regularity in the numerics. Appendix A details how accurate computations change the behavior of the Esipov-Shapiro system from what is presented in [16].

*Proteus mirabilis* swarm-colony development is important as a model system for other problems in morphology, complex self-organizing systems, and where spatial behavior is a manifestation of local kinetics. Not only are the choices made in the mathematical models important in this respect, but so is the computational framework used to solve them. One goal of this paper is to illustrate the necessity of robust and accurate new numerical methods in the modeling and solution of such systems.

The results of the numerical computations presented in Section 6 were obtained for the various parameter sets by using the age and space discretizations described in [2, 3] with time integration done using step-doubling extrapolation. Step-doubling is a time-stepping algorithm, going back to at least Gear [18] for ordinary differential equations, based on taking one step over a time interval to obtain one approximate solution for that interval, and then taking two half-steps over the same interval to get a second approximate solution. The two

solutions can then be compared for adaptive step-size control. Moreover, the two solutions can be combined to obtain a likely second-order approximation in time [4]. The use of a second-order adaptive method with error checking for these problems is important, since the front dynamics of a degenerate system can depend on the time step.

A uniform spatial discretization of size  $\Delta x = 1/300$ , and a uniform age discretization of  $\Delta a = 1/40$ , using piecewise constant basis functions, was sufficient to solve the system within a relative error in the  $L^2$ -norm of less than 1%. A uniform age discretization in the context of a moving grid method means that all but the first and last age intervals are constant in length, and that a new age interval is introduced at the birth boundary when the old birth interval reaches  $\Delta a$  in length. Convergence in time was obtained by adjusting a tolerance parameter for the adaptive time-stepping in the step-doubling algorithm so that the relative error in the  $L^2$ -norm was also less than 1%.

## 6 Results

We examine the response of the model to changes in the various parameters in the following tables. The spatial domain of the problems is  $\hat{r} \in [0, 1]$ , the temporal domain is truncated to the finite domain  $\hat{t} \in [0, 35]$ , and the age domain is  $\hat{a} \in [0, \hat{a}_{\max}]$ , which varies depending on the age of sharp septation in swarms.

The quantity  $T$  is the total time it takes for a swarm ring to form,  $S$  is the time spent in a swarm phase,  $C$  is the time spent in a consolidation phase, and  $R$  is the width of a swarm ring. Except for the parameter under study, the other parameters are set to  $\hat{a}_{\max} = 2.67$ ,  $V_c = 8$ ,  $D_0 = 2 \times 10^{-3}$ ,  $P_{\min} = 0.5$ ,  $\xi_0 = 0.5$ , and  $\hat{a}_{\min} = 0$ . In each of the tables, the default value of the parameter will be shown in bold type. Figure 1 shows the results of the model for the base parameters. The top graph is a three dimensional plot of the physical colony viewed from above and the bottom graph is a plot of colony radius versus time that

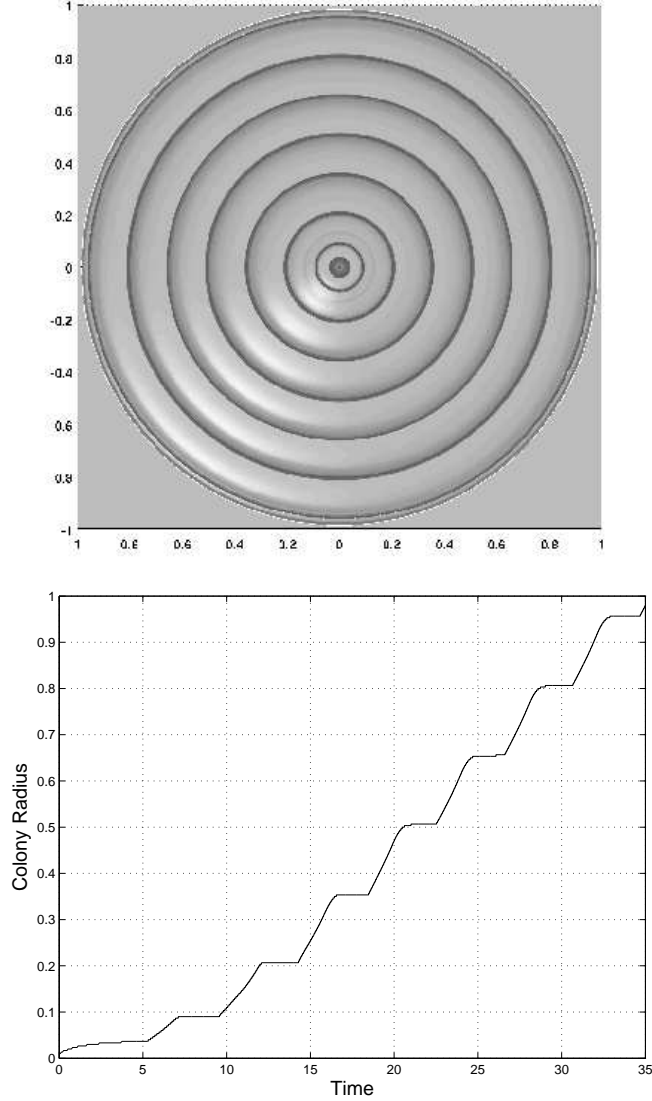


Figure 1: Computed *Proteus mirabilis* swarm colony with regularly spaced concentric terraces and periodic front velocity. The parameters for this swarm colony are  $\hat{a}_{\max} = 2.67$ ,  $V_c = 8$ ,  $D_0 = 2 \times 10^{-3}$ ,  $P_{\min} = 0.5$ ,  $\xi_0 = 0.5$ , and  $\hat{a}_{\min} = 0$ . The top figure is a 3D plot of the swarmer- and dividing-cell biomass viewed from directly above with a combination of ambient light, diffuse reflection, and specular reflection. The bottom figure shows the radius of the swarm colony as a function of time. Areas where the function has zero slope correspond to consolidation periods in the swarm-colony development. In dimensionless units, total time for the formation of one ring is  $T = 4.1$ , the time spent swarming is  $S = 2.2$ , the time spent in consolidation is  $C = 1.9$ , and the width of one ring is  $R = 0.153$ .

$\hat{a}_{\min}$	$T$	$S$	$C$	$S/C$	$R$	$R/S$
<b>0.0</b>	4.1	2.2	1.9	1.16	0.153	0.0695
0.5	4.1	2.0	2.1	0.95	0.150	0.0750
1.0	4.1	1.7	2.4	0.71	0.140	0.0824
2.0	4.1	1.3	2.8	0.46	0.090	0.0692

Table 2: Ring formation as a function of  $\hat{a}_{\min}$ .

$D_0$	$T$	$S$	$C$	$S/C$	$R$	$R/S$
0.001	4.05	2.15	1.9	1.13	0.107	0.0498
<b>0.002</b>	4.1	2.2	1.9	1.16	0.153	0.0695
0.003	4.1	2.3	1.8	1.28	0.183	0.0796
0.004	4.1	2.3	1.8	1.28	0.214	0.0930

Table 3: Ring formation as a function of  $D_0$ .

illustrates the periodic front dynamics of *Proteus* swarm-colony development.

Table 2 exhibits ring formation as a function of  $\hat{a}_{\min}$ , the minimum nondimensional age for a swarmer cell to contribute to swarming. The parameter  $\hat{a}_{\min}$  depends on agar concentration. As agar concentration increases, so does the difficulty of moving on the substrate, and hence  $\hat{a}_{\min}$  increases as well. As  $\hat{a}_{\min}$  increases,  $S$  and  $R$  decrease,  $C$  increases, and  $T$  stays the same. This is the response to increased agar concentrations seen in experiments; as agar concentration increases, swarm time and terrace width decrease, consolidation time increases, whereas total cycle time stays the same.

This invariance of the total time for ring formation,  $T$ , is further illustrated in Figure 2. A parameter similar to  $\hat{a}_{\min}$  controls the ratio of swarm time to consolidation time in [16]. Having averaged out the age variable, no such control is shown in [39].

Table 3 exhibits ring formation as a function of  $D_0$ , the constant of diffusion. The parameter  $D_0$  reflects changes in glucose concentration. The temporal metrics,  $T$ ,  $S$ , and  $C$ , change little, whereas there is significant change in the width of the terraces,  $R$ . This

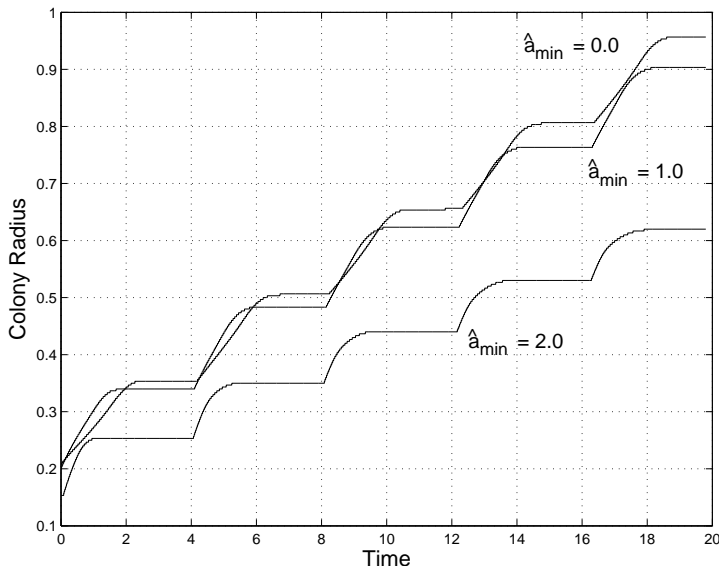


Figure 2: Swarm-colony front dynamics as a function of  $\hat{a}_{\min}$ . Shown are curves for the cases of  $\hat{a}_{\min} = 0.0$ ,  $\hat{a}_{\min} = 1.0$ , and  $\hat{a}_{\min} = 2.0$ . The other parameters for these swarm colonies are  $\hat{a}_{\max} = 2.67$ ,  $V_c = 8$ ,  $D_0 = 2 \times 10^{-3}$ ,  $P_{\min} = 0.5$ , and  $\xi_0 = 0.5$ . The curves have been realigned in time for better comparison of individual ring formation. Although total cycle time does not change, the ratio of time spent swarming to time spent in consolidation decreases as the minimum nondimensionalized age to contribute to swarming,  $\hat{a}_{\min}$ , increases.

corresponds to the experimental results illustrated in Figure 14 in [44], which shows minor variation in the total cycle time and the ratio of swarm to consolidation time, while showing a significant increase in terrace width.

Table 4 exhibits ring formation as a function of  $V_c$ , the nondimensionalized lag in the swarmer cell production,  $\xi$ . As  $V_c$  increases, we see an expected increase in the consolidation time,  $C$ . The time spent swarming,  $S$ , is nearly invariant. This leads to an increase in the overall cycle time,  $T$ , as  $V_c$  increases. The increased time building up swarmer rafts results in an increase in the front velocity,  $R/S$ , and thus in terrace width,  $R$ , as well.

The presence of a lag in swarmer-cell production was observed in [49]. However, the length of the lag, much less its explicit density dependence, is an open area of experimentation. The biological and chemical factors that underlie  $V_c$  are also unknown.

$V_c$	$T$	$S$	$C$	$S/C$	$R$	$R/S$
2	3.3	2.1	1.2	1.75	0.107	0.0510
4	3.6	2.2	1.4	1.57	0.133	0.0605
<b>8</b>	4.1	2.2	1.9	1.16	0.153	0.0695
16	4.5	2.2	2.3	0.96	0.157	0.0714

Table 4: Ring formation as a function of  $V_c$ .

$\xi_0$	$T$	$S$	$C$	$S/C$	$R$	$R/S$
0.25	4.7	1.65	3.05	0.54	0.067	0.0406
<b>0.50</b>	4.1	2.2	1.9	1.16	0.153	0.0695
0.75	3.7	2.6	1.1	2.40	0.230	0.0885
1.00	N/A	N/A	N/A	N/A	N/A	N/A

Table 5: Ring formation as a function of  $\xi_0$ .

Table 5 exhibits ring formation as a function of  $\xi_0$ , the constant of the differentiation ratio,  $\xi$ . The parameter  $\xi_0$  is clearly greater than zero, otherwise dividing cells would never beget swarms, and is thought to be less than one, as suggested in [49], “some of the cells near the perimeter of the colony begin to undergo a dramatic morphological change to highly elongated forms...” Results for  $\xi_0 = 1$  show the loss of a swarming consolidation cycle and a nearly constant rate of colony expansion.

As  $\xi_0$  increases, the consequent increase in swarmer-cell production results in longer time spent swarming,  $S$ , and terrace width,  $R$ , but a decrease in total cycle time,  $T$ , and consolidation time,  $C$ .

Table 6 exhibits ring formation as a function of  $P_{\min}$ , the minimum swarmer biomass for swarming to begin. The parameter  $P_{\min}$  reflects the need for swarmers to build “rafts” with other swarmers in order to move. “Movement of individual cells seems to be retarded whereas cells moving in larger groups do so much more effectively” [49]. Rafts are able to form in sufficient numbers only when there is a minimum swarmer biomass present. The

$P_{\min}$	$T$	$S$	$C$	$S/C$	$R$	$R/S$
0.0	4.3	N/A	N/A	N/A	0.186	N/A
0.2	4.2	2.8	1.4	2.00	0.170	0.0607
0.3	4.15	2.6	1.55	1.68	0.163	0.0627
<b>0.5</b>	4.1	2.2	1.9	1.16	0.153	0.0695
0.7	3.95	2.05	1.9	1.08	0.140	0.0683
1.0	3.85	1.9	1.95	0.97	0.127	0.0668

Table 6: Ring formation as a function of  $P_{\min}$ .

$\hat{a}_{\max}$	$T$	$S$	$C$	$S/C$	$R$	$R/S$
2.00	3.8	1.5	2.3	0.65	0.090	0.0600
2.33	3.9	1.8	2.1	0.86	0.120	0.0667
<b>2.67</b>	4.1	2.2	1.9	1.16	0.153	0.0695
3.00	4.25	2.5	1.75	1.43	0.190	0.0760
3.50	4.5	3.2	1.3	2.46	0.253	0.0791

Table 7: Ring formation as a function of  $\hat{a}_{\max}$ .

parameter  $P_{\min}$  differs from  $\hat{a}_{\min}$  in that it is a measure of weighted population density rather than of the size of an individual. It is unclear what biological or chemical factors set the minimum swarmer biomass, or even if this threshold differs substantially as experimental parameters vary.

As  $P_{\min}$  increases, the total time spent swarming,  $S$ , decreases, and the time spent in consolidation,  $C$  increases. This is the same as the response of the system to changes in  $\hat{a}_{\min}$ , except that the total cycle time,  $T$ , remains strongly invariant under changes in  $\hat{a}_{\min}$ , but decreases somewhat as  $P_{\min}$  increases. The terrace width,  $R$ , decreases as  $P_{\min}$  increases, as it does with increases in  $\hat{a}_{\min}$ .

The parameter  $P_{\min}$  is needed in the models to generate a distinct consolidation phase. The loss of a clear distinction between swarming and consolidation as  $P_{\min}$  goes to zero is further illustrated in Figure 3.

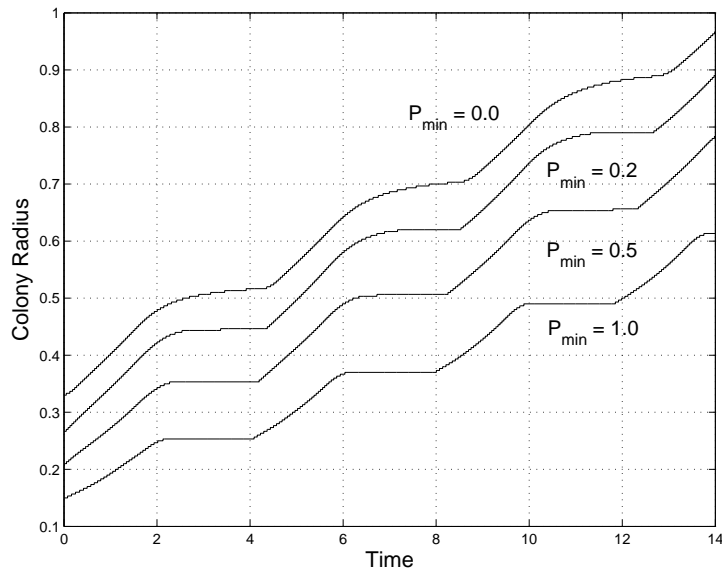


Figure 3: Swarm-colony front dynamics as a function of  $P_{\min}$ . Shown are curves for the cases of  $P_{\min} = 0.0$ ,  $P_{\min} = 0.2$ ,  $P_{\min} = 0.5$ , and  $P_{\min} = 1.0$ . The other parameters for these swarm colonies are  $\hat{a}_{\max} = 2.67$ ,  $V_c = 8$ ,  $D_0 = 2 \times 10^{-3}$ ,  $\hat{a}_{\min} = 0.0$ , and  $\xi_0 = 0.5$ . The curves have been realigned in time for better comparison of individual ring formation. This figure illustrates the loss of a distinct transition from swarming to consolidation phase as  $P_{\min}$  goes to zero.

Table 7 exhibits ring formation as a function of  $\hat{a}_{\max}$ , the dimensionless age at which a multinuclear swarmer cell breaks down into mononuclear dividing cells. A swarm colony with larger swarmer cells, i.e. larger  $\hat{a}_{\max}$ , can be expected to have longer swarming phases,  $S$ , with wider terrace widths,  $R$ . The total cycle time,  $T$ , is also seen to increase as  $\hat{a}_{\max}$  increases, whereas the time spent in consolidation,  $C$ , decreases.

## 7 Conclusions

In this paper we have presented models and computational results to understand the periodic front dynamics in *Proteus mirabilis* swarm-colony development. These models differ from previous work by placing the most emphasis on known biological mechanisms, in particular the local kinetics, or age-structure, and make fewer assumptions about the diffusivity. The numerical solutions to the model show the periodicity seen in the biological system, as well as the invariance of the cycle time to parameters sensitive to changes in agar and glucose concentration, and retain a mechanism for controlling the ratio of swarm to consolidation time within an invariant total cycle time. These results were obtained by robust and accurate numerical methods designed specifically for age-structured diffusion problems, with proven convergence properties.

Future work on further understanding *Proteus* swarm-colony development includes experimental studies on the forms of the differentiation function,  $\xi$ . Experiments to determine how differentiation from dividing cells to swarmer cells depends on local population density would be particularly valuable.

Other areas of future research are the specifics of how the much larger and broader issue of biological motion relates to *Proteus* motion on an agar surface, and modeling the effects of a non-sharp age of septation on the regularity of *Proteus* front dynamics. Extending the models to explicit two-dimensional space to understand the interaction of multiple colonies

is also an area of future research.

*Proteus mirabilis* should be seen as a model system with relevance to other biological problems. The further mathematical understanding of age and space structured models – and the numerics to solve them – constitutes an important foundational area of research.

## Acknowledgements

The author thanks James Shapiro at the University of Chicago for introducing him to *Proteus mirabilis*. The author has had many helpful discussions with Todd F. Dupont, Tasso Kaper, Nancy Kopell, Mitsugu Matsushita, Georgiy Medvedev, Thomas Nagylaki, and Oliver Rauprich.

## A Numerical Solutions of the Esipov-Shapiro Model

The Esipov-Shapiro model, as described by the relevant equations and parameters in [16], has no spatial dynamics whatsoever.

We make several natural changes in the Esipov-Shapiro model to generate something resembling *Proteus mirabilis* swarm-colony development. These changes, although not contained in their equations, are suggested in the text.

We set the units of the parameter  $D_0$  to  $\text{cm}^2/\text{hr}$  rather than  $\text{cm}^2/\text{sec}$ . Use of the latter causes very rapid swarming that covers the entire domain in a short time. It is reasonable to believe that this is a typo, as all other parameters in [16] use hours as the time unit. The second change is the use of swarmer biomass rather than numerical density as the relevant measure of total population. Although the formal mathematical definition of  $P_s$  (page 255 of [16]) is given by  $P_s = \int_{\theta_{\min}}^{\theta_{\max}} d\theta \rho_s(\mathbf{r}, \theta, t)$ , the statement at the top of page 253,

Surface densities of swimmer and swarmer cell populations will be indicated

by the capital letters  $P_c$  and  $P_s$ , respectively ( $c$  for consolidation phase,  $s$  for swarming phase). While we do not resolve swimmers in age, the surface density of swimmers is related to a biomass weighted average over the ages, with  $e^{\theta/\tau_d}$  being the contribution of age  $\theta$ .

along with personal communication with Sergei Esipov (July, 1997), and the statement by the authors in [44] that their models in [16] use an “age-weighted swarmer cell density”, indicates that a mass-weighted  $P_s$  was used in their numerical computations. This is a necessary reinterpretation. The use of a non-weighted  $P_s$  precludes the upper trigger of the memory field needed to instigate swarming,  $P_{s,\max}$ , from ever being reached, which in turn results in no swarm-colony development whatsoever.

Another change in the Esipov-Shapiro model needed to get some sort of swarming and consolidation behavior is the incorporation of what they refer to as the “drivers license” age,  $\theta_{\min}$ , explicitly into the diffusivity. As the equations are written,  $\theta_{\min}$  enters the system implicitly only through the definition of  $P_s$ . Thus, small swimmers move with larger swimmers in the “rafts”; they just do not contribute to a raft’s motility. This is a reasonable assumption – nothing prevents them from being caught up in the flow – and one made in the models presented in this paper. But because we use a lag phase in septation, the presence or absence of “underage” swimmers in rafts does not qualitatively affect our model. However, since it does not contain such a lag, the Esipov-Shapiro model does not develop a consolidation phase after the first swarm phase, but rather the swimmers develop a self-sustaining soliton caused by swimmers of maximum age that dedifferentiate into swimmers (dividing cells,) immediately differentiating into new swimmers. Although this does not reflect the observed behavior of *Proteus*, it is an interesting mathematical object, which we display in Figure 4.

If we reinterpret the meaning of the “drivers license” age to be that small swimmers do not move at all, we need to multiply the diffusivity,  $D$ , as written in Equation (4a) on

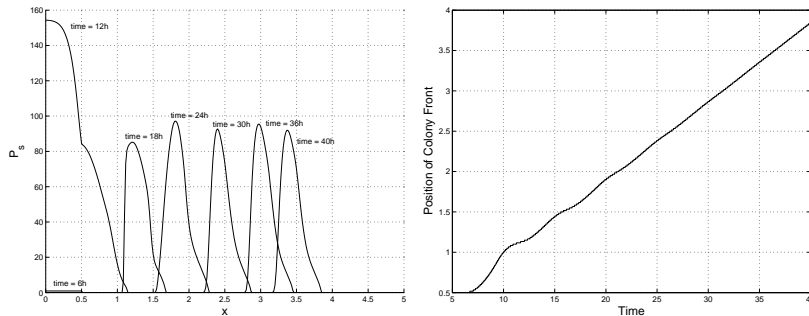


Figure 4: Profiles of swarmer biomass for the Esipov-Shapiro model without  $\Theta(\theta_{\min})$  in the diffusivity. The model does not develop a consolidation phase after the first swarm phase, but rather the swarmer develop a self-sustaining soliton where swarmer of maximum age that dedifferentiate into dividing cells immediately differentiate into new swarmer. The parameters used in this computation are taken from the caption of Figure 4 in [16], with the choice of  $D_0 = 0.045$ .

page 256 of [16], by the Heaviside function  $\Theta(\theta_{\min})$ . Doing so results in a system with a swarming/consolidation cycle with fixed time lengths, but not the regularly spaced terraces seen in the experiments. The terrace widths decrease in length each cycle. This is illustrated for several values of  $D_0$  in the Esipov-Shapiro model in Figure 5.

The cause of the spatial regularity seen in the computations in [16] is quite possibly due to computational effects. The numerical integration in age and time in [16] is not done along characteristics, but rather consists of transforming age to a stage-structured variable dependent upon discretization parameters, adding regularity to a system that is not really there. Another possible source of error is that the space and time integration, as written in Equations (6b)-(6d) on page 257 of [16], has the property that the colony front can move at most one spatial interval per time step. Thus, inaccurate numerics can change the nature of the bacterial front.

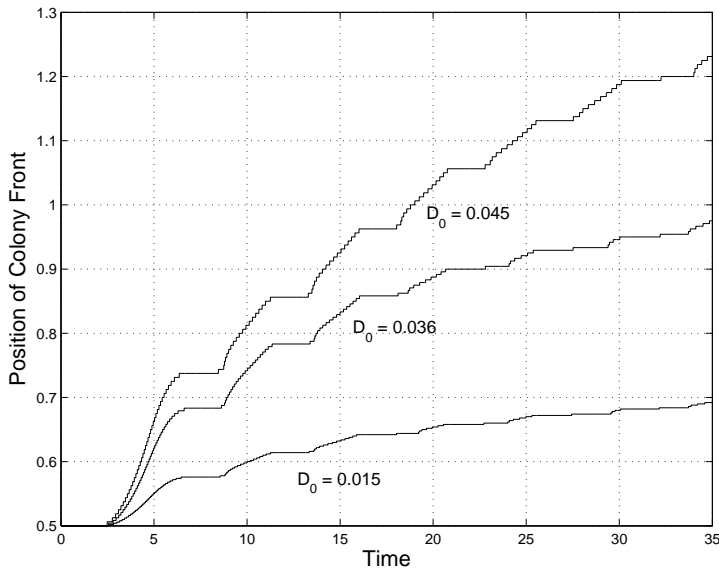


Figure 5: Swarm-colony front dynamics of the Esipov-Shapiro model as a function of their  $D_0$ . The parameters used in these computations are taken from the caption of Figure 4 in [16], including the choice of  $D_0 = (0.045, 0.036, 0.015)$ .

## B Use of Different Forms of $\xi$

We chose a smooth piecewise cubic function for the form of  $\xi$  in Equation (4.1i) for numerical reasons. In this appendix, we argue that it is the lag in  $\xi$ , not the shape of the curve, that is relevant in modeling *Proteus* swarm-colony development. We present two sets of results from using two different piecewise constant functions with the same area under the curve as the piecewise cubic. The first, “fat” one,

$$\xi_f(v) = \begin{cases} \frac{1}{2}\xi_0, & |v - v_c| \leq v_w, \\ 0, & \text{otherwise,} \end{cases} \quad (\text{B.5})$$

has the same support, but shorter maximum height, than the cubic. The second, “skinny” one,

$$\xi_s(v) = \begin{cases} \xi_0, & |v - v_c| \leq \frac{1}{2}v_w, \\ 0, & \text{otherwise,} \end{cases} \quad (\text{B.6})$$

$V_c$	$T$	$S$	$C$	$R$
2	3.3	2.1	1.2	0.097
4	3.7	2.1	1.6	0.120
<b>8</b>	4.1	2.1	2.0	0.131
16	4.7	2.1	2.6	0.134

Table 8: Ring formation as a function of  $V_c$  using Equation (B.5).

$V_c$	$T$	$S$	$C$	$R$
2	3.2	2.2	1.0	0.117
4	3.5	2.3	1.2	0.147
<b>8</b>	4.0	2.3	1.7	0.164
16	4.5	2.3	2.2	0.176

Table 9: Ring formation as a function of  $V_c$  using Equation (B.6).

has the same maximum height, but narrower support, than the cubic. Using Equation (B.5) instead of Equation (4.1i) gives Table 8 in place of the same data in Table 4. Using Equation (B.6) instead of Equation (4.1i) gives Table 9 in place of those data in Table 4.

The temporal and spatial regularity seen in *Proteus* and the computations presented earlier with a piecewise cubic  $\xi$  are also present in these computations. These results indicate that changing the form of  $\xi$  does not alter the qualitative behavior of the system and has only a minor quantitative effect on the solutions. Nonetheless, the shape of  $\xi$ , and not only its mass and support, is an interesting topic for experiments.

## References

- [1] D. G. ARONSON, *The role of diffusion in mathematical population biology: Skellam revisited*, in Mathematics in Biology and Medicine, V. Capasso, E. Grosso, and S. L. Paveri-Fontana, eds., vol. 57 of Lecture Notes in Biomathematics, Springer-Verlag, Berlin, 1985, pp. 2–6.

- [2] B. P. AYATI, *A variable time step method for an age-dependent population model with nonlinear diffusion*, SIAM J. Numer. Anal., 37 (2000), pp. 1571–1589.
- [3] B. P. AYATI AND T. F. DUPONT, *Galerkin methods in age and space for a population model with nonlinear diffusion*, SIAM J. Numer. Anal., 40 (2002), pp. 1064–1076.
- [4] ———, *Convergence of a step-doubling Galerkin method for parabolic problems*, Math. Comp., posted electronically September 10, 2004, to appear in print. (2004).
- [5] N. BELLOMO AND L. PREZIOSI, *Modelling and mathematical problems related to tumor evolution and its interaction with the immune system*, Mathematical and Computer Modelling, 32 (2000), pp. 413–452.
- [6] A. BERTUZZI AND A. GANDOLFI, *Cell kinetics in a tumor cord*, J. Theo. Biol., 204 (2000), pp. 587–599.
- [7] B. M. BOLKER, S. W. PACALA, AND C. NEUHAUSER, *Spatial dynamics in model plant communities: What do we really know?*, American Naturalist, 162 (2003), pp. 135–148.
- [8] S. BUSENBERG AND M. IANNELLI, *A class of nonlinear diffusion problems in age-dependent population dynamics*, Nonlin. Anal. Th. Meth. Appl., 7 (1983), pp. 501–529.
- [9] C. CHIU, *A numerical method for nonlinear age dependent population models*, Diff. Int. Eqns., 3 (1990), pp. 767–782.
- [10] A. M. DE ROOS, *Numerical methods for structured population models: The escalator boxcar train*, Num. Meth. Part. Diff. Eqns., 4 (1989), pp. 173–195.
- [11] ———, *A gentle introduction to physiologically structured population models*, in Structured-population Models in Marine, Terrestrial, and Freshwater Systems, S. Tul-

japurkar and H. Caswell, eds., vol. 18 of Population and Community Biology Series, Chapman & Hall, New York, 1997, ch. 5, pp. 119–204.

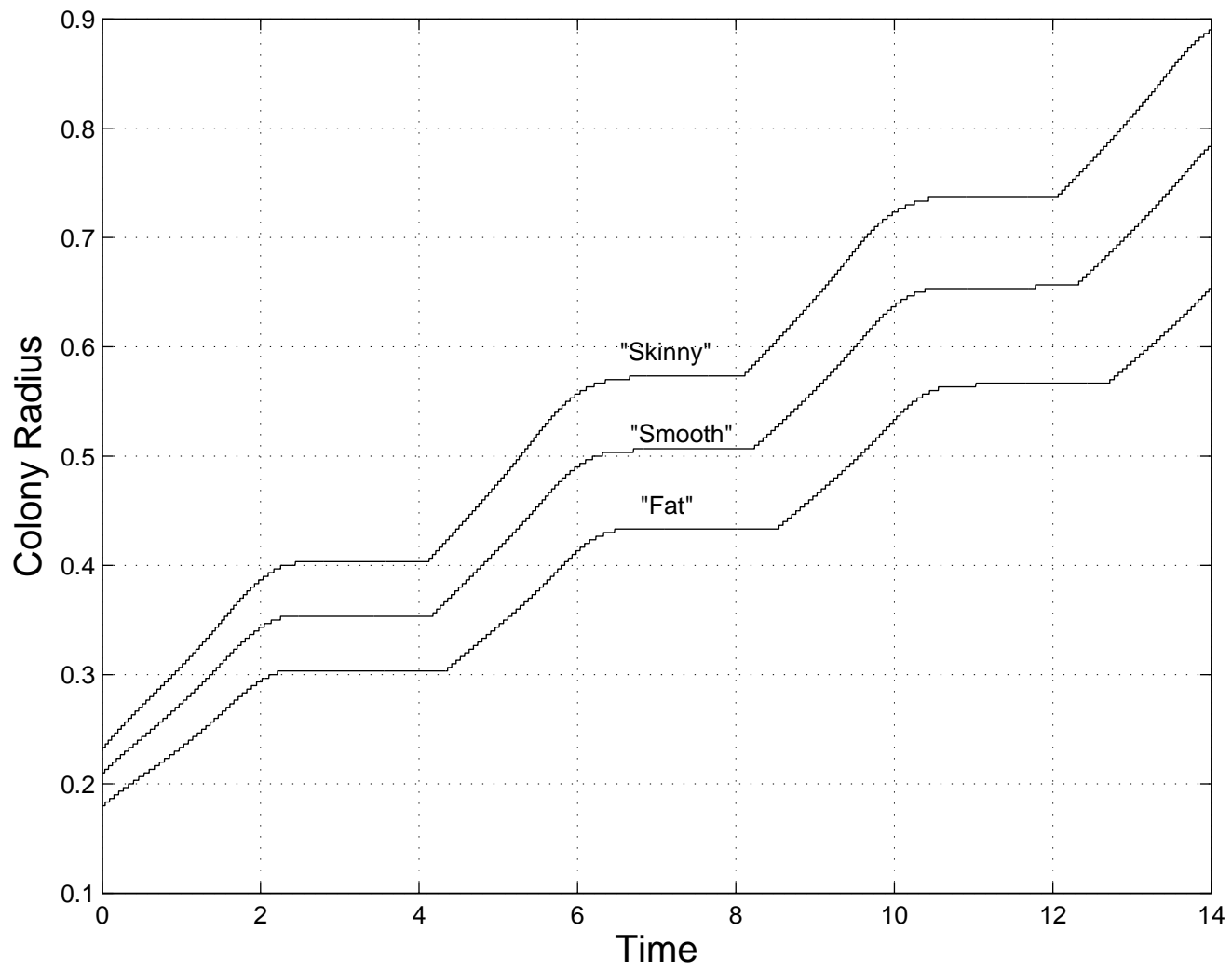
- [12] A. M. DE ROOS AND J. A. J. METZ, *Towards a numerical analysis of the escalator boxcar train*, in Differential Equations with Applications in Biology, Physics and Engineering, J. A. Goldstein, F. Kappel, and W. Schappacher, eds., vol. 133 of Lecture Notes in Pure and Applied Mathematics, Marcel Dekker, New York, 1991, pp. 91–113.
- [13] G. DI BLASIO, *Non-linear age-dependent population diffusion*, J. Math. Bio., 8 (1979), pp. 265–284.
- [14] G. DI BLASIO AND L. LAMBERTI, *An initial-boundary problem for age-dependent population diffusion*, SIAM J. Appl. Math., 35 (1978), pp. 593–615.
- [15] J. DYSON, R. VILLELLA-BRESSAN, AND G. F. WEBB, *Asynchronous exponential growth in an age structured population of proliferating and quiescent cells*, Math. Biosci., 177-178 (2002), pp. 73–83.
- [16] S. E. ESIPOV AND J. A. SHAPIRO, *Kinetic model of Proteus mirabilis swarm colony development*, J. Math. Biol., 36 (1998), pp. 249–268.
- [17] G. FAIRWEATHER AND J. C. LÓPEZ-MARCOS, *A box method for a nonlinear equation of population dynamics*, IMA J. Numer. Anal., 11 (1991), pp. 525–538.
- [18] C. W. GEAR, *Numerical Initial Value Problems in Ordinary Differential Equations*, Prentice–Hall, New Jersey, 1971.
- [19] M. E. GURTIN, *A system of equations for age-dependent population diffusion*, J. Theor. Biol., 40 (1973), pp. 389–392.

- [20] M. E. GURTIN AND R. C. MACCAMY, *Non-linear age-dependent population dynamics*, Arch. Rat. Mech. Anal., 54 (1974), pp. 281–300.
- [21] ———, *Diffusion models for age-structured populations*, Math. Biosci., 54 (1981), pp. 49–59.
- [22] T. HÖFER, J. A. SHERRATT, AND P. K. MAINI, *Cellular pattern formation during Dictostelium aggregation*, Physica D, 85 (1995), pp. 425–444.
- [23] C. HUANG, *An age-dependent population model with nonlinear diffusion in  $\mathbb{R}^n$* , Quart. Appl. Math., 52 (1994), pp. 377–398.
- [24] E. L. IONIDES, K. S. FANG, R. R. ISSEROFF, AND G. F. OSTER, *Stochastic models for cell motion and taxis*, J. Math. Biol., 48 (2004), pp. 23–37.
- [25] M.-Y. KIM, *Galerkin methods for a model of population dynamics with nonlinear diffusion*, Num. Meth. Part. Diff. Eqns., 12 (1996), pp. 59–73.
- [26] M.-Y. KIM AND E.-J. PARK, *Mixed approximation of a population diffusion equation*, Computers Math. Applic., 30 (1995), pp. 23–33.
- [27] T. KOHYAMA, *Size-structured multi-species model of rain forest trees*, Functional Ecology, 6 (1992), pp. 206–212.
- [28] ———, *Size-structured tree populations in gap-dynamic forest – the forest architecture hypothesis for the stable coexistence of species*, J. Ecology, 81 (1993), pp. 131–143.
- [29] B. W. KOOI AND S. A. L. M. KOOLJMAN, *Discrete event versus continuous approach to reproduction in structured population dynamics*, Theo. Popul. Biol., 56 (1999), pp. 91–105.

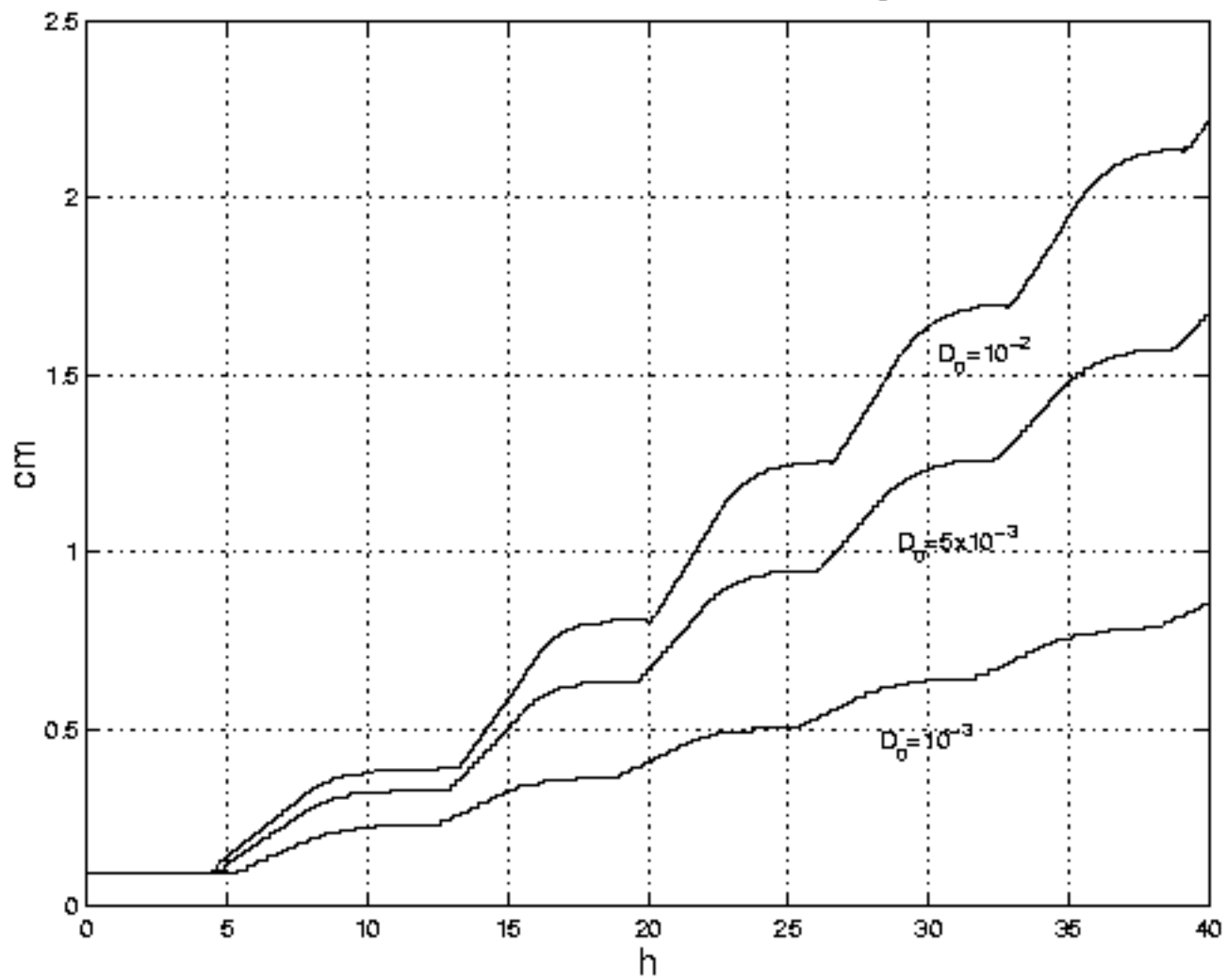
- [30] M. A. KRAEMER, L. V. KALACHEV, AND D. W. COBLE, *A class of models describing age structure dynamics in a natural forest*, *Natural Resource Modeling*, 15 (2002), pp. 149–200.
- [31] K. KUBO AND M. LANGLAIS, *Periodic solutions for a population dynamics problem with age-dependence and spatial structure*, *J. Math. Biol.*, 29 (1991), pp. 363–378.
- [32] Y. KWON AND C.-K. CHO, *Second-order accurate difference methods for a one-sex model of population dynamics*, *SIAM J. Numer. Anal.*, 30 (1993), pp. 1385–1399.
- [33] M. LANGLAIS, *A nonlinear problem in age-dependent population diffusion*, *SIAM J. Math. Anal.*, 16 (1985), pp. 510–529.
- [34] ———, *Large time behavior in a nonlinear age-dependent population dynamics problem with spatial diffusion*, *J. Math. Biol.*, 26 (1988), pp. 319–346.
- [35] L. LOPEZ AND D. TRIGIANTE, *A finite difference scheme for a stiff problem arising in the numerical solution of a population dynamic model with spatial diffusion*, *Nonlin. Anal. Th. Meth. Appl.*, 9 (1985), pp. 1–12.
- [36] J. C. LÓPEZ-MARCOS, *An upwind scheme for a nonlinear hyperbolic integro-differential equation with integral boundary condition*, *Computers Math. Applic.*, 22 (1991), pp. 15–28.
- [37] R. C. MACCAMY, *A population model with nonlinear diffusion*, *J. Diff. Eqns.*, 39 (1981), pp. 52–72.
- [38] P. MARCATI, *Asymptotic behavior in age-dependent population dynamics with hereditary renewal law*, *SIAM J. Math. Anal.*, 12 (1981), pp. 904–916.

- [39] G. S. MEDVEDEV, T. J. KAPER, AND N. KOPELL, *A reaction-diffusion equation with periodic front dynamics*, SIAM J. Appl. Math., 60 (2000), pp. 1601–1638.
- [40] J. D. MURRAY, *Mathematical Biology II: Spatial Models and Biomedical Applications*, vol. 18 of Interdisciplinary Applied Mathematics, Springer–Verlag, Berlin, third ed., 2003.
- [41] T. NAGYLAKI, *The diffusion model for migration and selection*, in Some Mathematical Questions in Biology: Models in Population Biology, A. Hastings, ed., vol. 20 of Lectures on Mathematics in the Life Sciences, American Mathematical Society, Providence, R.I., 1989, pp. 55–75.
- [42] M. PASCUAL AND S. A. LEVIN, *Spatial scaling in a benthic population model with density-dependent disturbance*, Theor. Popul. Biol., 56 (1999), pp. 106–122.
- [43] L. PREZIOSI, ed., *Cancer Modelling and Simulation*, Chapman & Hall/CRC, 2003.
- [44] O. RAUPRICH, M. MATSUSHITA, K. WEIJER, F. SIEGERT, S. E. ESIPOV, AND J. A. SHAPIRO, *Periodic phenomena in *Proteus mirabilis* swarm colony development*, J. Bacteriol., 178 (1996), pp. 6525–6538.
- [45] M. ROTENBERG, *Theory of population transport*, J. Theor. Biol., 37 (1972), pp. 291–305.
- [46] J. G. SKELLAM, *Random dispersal in theoretical populations*, Biometrika, 38 (1951), pp. 196–218.
- [47] D. SULSKY, *Numerical solution of structured population models, I. age structure*, J. Math. Biol., 31 (1993), pp. 817–839.

- [48] G. F. WEBB, *Theory of Nonlinear Age-dependent Population Dynamics*, vol. 89 of Pure and Applied Mathematics, Marcel Dekker, New York, 1985.
- [49] F. D. WILLIAMS AND R. H. SCHWARZHOFF, *Nature of the swarming phenomenon in Proteus*, Ann. Rev. Microbiol., 32 (1978), pp. 101–122.



Front Position. Variation of  $D_0$



Front Position. Variation of  $D_0$ . Fickian Diffusion

